The Canadian Mineralogist
Vol. 42, pp. 797-806 (2004)

THE CRYSTAL CHEMISTRY OF EPISTOLITE

Elena SOKOLOVA[§] and Frank C. HAWTHORNE

Department of Geological Sciences, University of Manitoba, Winnipeg, Manitoba R3T 2N2, Canada

Abstract

The crystal structure of epistolite, ideally $Na_4\,Nb_2\,Ti^{4+}\,(Si_2O_7)_2\,O_2\,(OH)_2\,(H_2O)_4$, *a* 5.460(1), *b* 7.170(1), *c* 12.041(2) Å, α 103.63(3), β 96.01(3), γ 89.98(3)°, *V* 455.4(5) Å^3, space group $P\bar{1}$, *Z* = 1, D_{calc} 2.987 g.cm^{-3} from the Ilímaussaq alkaline complex, South Greenland, has been solved by direct methods and refined to R_1 9.8% on the basis of 1986 unique reflections $|F_o \geq 4\sigma F|$ collected on a Bruker *P*4 diffractometer with a CCD 1K Smart detector and Mo*K*α radiation. An electron-microprobe analysis gave (wt.%): SiO_2 29.59, Nb_2O_5 31.43, TiO_2 10.24, MnO 0.34, Fe_2O_3 0.35, Ta_2O_5 0.28, Na_2O 14.45, CaO 1.89 K_2O 0.27, P_2O_5 0.36, F 1.32, H_2O (calculated from structure refinement) 10.46, total 100.43. The empirical formula is $(Na_{3.79}\,Ca_{0.27}\,Mn_{0.04})_{\Sigma 4.06}\,(Nb_{1.92}\,Ti^{4+}_{0.04}\,Fe^{3+}_{0.04})_{\Sigma 2.00}\,Ti^{4+}\,(Si_2O_7)_2\,O_2\,(OH_{1.44}\,F_{0.56})\,(H_2O)$, calculated on the basis of 4 Si (*apfu*). In the crystal structure, there are two tetrahedrally coordinated sites occupied by Si, with a grand <Si–O> distance of 1.617 Å. The (SiO_4) tetrahedra link together to form $[Si_2O_7]$ groups. There are two octahedrally coordinated *M* sites. The *M*(1) site is occupied primarily by Nb with minor amounts of Fe^{3+} and Ti^{4+}, with <*M*(1)–O, H_2O> = 2.01 Å. The *M*(2) site is occupied solely by Ti^{4+}, with <*M*(2)–O,OH> = 1.962 Å. There are three *A* sites, occupied primarily by Na: the *A*(1) and *A*(2) sites are octahedrally coordinated, with <*A*(1,2)–O,OH> = 2.39 Å, and the *A*(3) site is [8]-coordinated, with <*A*(3)–O,OH,H_2O> = 2.57 Å. The *A*(1) site is occupied by Na, the *A*(2) site is occupied 92% by Na, and the *A*(3) site is approximately half-occupied by Na: $0.87\,Na + 0.82\,\square + 0.27\,Ca + 0.04\,Mn^{2+}$ *apfu*. The *M*(2) and *A*(1,2) octahedra each share six common edges to form a close-packed sheet. This sheet of octahedra is the central part of a *TS* (titanium-silicate) block. Two adjacent sheets of heteropolyhedra consist of $[Si_2O_7]$ groups and *M*(1) octahedra with large hexagonal voids that incorporate [8]-coordinated *A*(3) polyhedra. A sheet of heteropolyhedra is connected to a sheet of octahedra through vertices of (SiO_4) tetrahedra, *M*(1) octahedra and *A*(3) polyhedra. Within one *TS* block in epistolite, two $[Si_2O_7]$ groups, one from each sheet of heteropolyhedra, link to the *M*(2) octahedron of the central sheet, and sheets of heteropolyhedra are approximately related by a pseudo-mirror plane, m_z. The *TS* blocks repeat along (001) and are connected through hydrogen bonds involving (H_2O) groups and acceptor O atoms of the *TS* blocks. Previously, the crystal structure of murmanite, ideally $Na_4\,Ti^{4+}_4\,(Si_2O_7)_2\,O_4\,(H_2O)_4$, *a* 5.383(4), *b* 7.053(4), *c* 12.170(3) Å, α 93.16(2), β 107.82(2), γ 90.06(2)°, *V* 439.14 Å^3, space group *P*1, *Z* = 1, D_{calc} 2.86 g cm^{-3}, has been considered as a topological analogue of epistolite. It has a *TS* block as a fundamental building block, but its bond topology is different from that in epistolite. This difference results from different linkages between the central sheet of octahedra and the two adjacent sheets of heteropolyhedra. In murmanite, sheets of heteropolyhedra are shifted relative to each other in the (001) plane. Thus epistolite and murmanite are not isostructural. Murmanite and epistolite are related by the substitution $Ti^{4+}_3 + O^{2-}_2 \leftrightarrow Nb^{5+}_2 + \square + (OH)^-_2$.

Keywords: epistolite, crystal structure, disorder, murmanite, Ilímaussaq alkaline complex, South Greenland.

Sommaire

Nous avons résolu la structure cristalline de l'épistolite, de formule idéale $Na_4\,Nb_2\,Ti^{4+}\,(Si_2O_7)_2\,O_2\,(OH)_2\,(H_2O)_4$, *a* 5.460(1), *b* 7.170(1), *c* 12.041(2) Å, α 103.63(3), β 96.01(3), γ 89.98(3)°, *V* 455.4(5) Å^3, groupe spatial $P\bar{1}$, *Z* = 1, D_{calc} 2.987 g.cm^{-3}, provenant du complexe alcalin d'Ilímaussaq, dans le sud du Groënland, par méthodes directes, et nous l'avons affinée jusqu'à un résidu R_1 de 9.8% en utilisant 1986 réflexions uniques $|F_o \geq 4\sigma F|$ prélevées avec un diffractomètre Bruker *P*4 muni d'un détecteur CCD 1K (rayonnement Mo*K*α). Une analyse avec une microsonde électronique a donné (proportions pondérales): SiO_2 29.59, Nb_2O_5 31.43, TiO_2 10.24, MnO 0.34, Fe_2O_3 0.35, Ta_2O_5 0.28, Na_2O 14.45, CaO 1.89 K_2O 0.27, P_2O_5 0.36, F 1.32, H_2O (quantité calculée à partir le l'affinement de la structure) 10.46, pour un total de 100.43. La formule empirique est $(Na_{3.79}\,Ca_{0.27}\,Mn_{0.04})_{\Sigma 4.06}\,(Nb_{1.92}\,Ti^{4+}_{0.04}\,Fe^{3+}_{0.04})_{\Sigma 2.00}\,Ti^{4+}\,(Si_2O_7)_2\,O_2\,(OH_{1.44}\,F_{0.56})\,(H_2O)$; elle est calculée sur une base de 4 Si (*apfu*). La structure contient de sites tétraédriques qu'occupe le Si, avec une distance globale <Si–O> de 1.617 Å. Les tétraèdres (SiO_4) sont agencés en groupes $[Si_2O_7]$. Il y a deux sites *M* à coordinence octaédrique. Le site *M*(1) contient surtout le Nb, avec des quantités moindres de Fe^{3+} et Ti^{4+}, et <*M*(1)–O, H_2O> est égal à 2.01 Å. Le site *M*(2) ne contient que le Ti^{4+}, avec <*M*(2)–O,OH> = 1.962 Å. Il y a trois sites *A*, qui contiennent surtout le Na; les sites *A*(1) et *A*(2) ont une coordinence octaédrique, avec <*A*(1,2)–O,OH> = 2.39 Å, et le site *A*(3) possède une coordinence [8], avec <*A*(3)–O,OH,H_2O> = 2.57 Å. Le site *A*(1) contient uniquement le Na, le site *A*(2) en contient à 92%, et le site *A*(3) est environ à moitié rempli par le Na: $0.87\,Na + 0.82\,\square + 0.27\,Ca + 0.04\,Mn^{2+}$ *apfu*. Les sites

---

[§] *E-mail address*: elena_sokolova@umanitoba.ca

octaédriques *M*(2) et *A*(1,2) partagent six arêtes communes pour former un feuillet à empilement compact. Ce feuillet d'octaèdres constitue l'élément central d'un bloc *TS* (à silicate de titanium). Deux feuillets adjacents d'hétéropolyèdres consistent de groupes $[Si_2O_7]$ et d'octaèdres *M*(1) parmi lesquels de grosses cavités hexagonales renferment les polyèdres *A*(3) à coordinence [8]. Un feuillet d'hétéropolyèdres est connecté à un feuillet d'octaèdres par les vertex des tétraèdres (SiO_4), des octaèdres *M*(1) et des polyèdres *A*(3). A l'intérieur d'un bloc *TS* dans l'épistolite, deux groupes $[Si_2O_7]$, un de chaque feuillet d'hétéropolyèdres, sont connectés à l'octaèdre *M*(2) du feuillet central, et les feuillets d'hétéropolyèdres sont *grosso modo* agencés selon un pseudo-mirroir m_z. Les blocs *TS* se répètent le long de (001) et sont connectés grâce à des liaisons hydrogène impliquant des groupes (H_2O) et des atomes accepteurs d'oxygène des blocs *TS*. On avait considéré la structure cristalline de la murmanite, de formule idéale $Na_4\ Ti^{4+}_4\ (Si_2O_7)_2\ O_4\ (H_2O)_4$, *a* 5.383(4), *b* 7.053(4), *c* 12.170(3) Å, α 93.16(2), β 107.82(2), γ 90.06(2)°, *V* 439.14 Å^3, groupe spatial *P*1, *Z* = 1, D_{calc} 2.86 g cm^{-3}, comme l'analogue topologique de l'épistolite. La murmanite contient aussi le bloc *TS* comme unité fondamentale, mais la topologie des liaisons diffère de celle de l'épistolite. Cette différence est le résultat d'agencements différents entre le feuillet central d'octaèdres et des deux feuillets adjacents d'hétéropolyèdres. Dans la murmanite, les feuillets d'hétéropolyèdres sont déplacés l'un l'autre dans le plan (001). L'épistolite et la murmanite ne sont donc pas isostructurales. Ces phases sont liées par la substitution $Ti^{4+}_3 + O^{2-}_2 \leftrightarrow Nb^{5+}_2 + \square + (OH)^-_2$.

(Traduit par la Rédaction)

Mots-clés: épistolite, structure cristalline, désordre, murmanite, complexe alcalin d'Ilímaussaq, Groënland du Sud.

INTRODUCTION

Epistolite is a low-temperature (Nb–Ti)-silicate mineral first described from the Ilímaussaq alkaline complex in South Greenland (Bøggild 1901), and then found in the Lovozero alkaline massif, Kola Peninsula, Russia (Semenov *et al.* 1962). The crystal structure of epistolite was proposed by Khalilov (1965) and Khalilov *et al.* (1965b: *a* 5.41, *b* 7.08, *c* 12.07 Å, α 103.1, β 96.1, γ 88.0°, space group *P*1), and this version has been the accepted structure of epistolite since then. Khalilov *et al.* (1965b) presented a drawing of a two-dimensional projection of the crystal structure of epistolite with an R_{h0l} = 22%, but gave no atom coordinates for the structure. Based on the structure of murmanite (Khalilov *et al.* 1965a, *a* 5.50, *b* 7.00, *c* 11.94 Å, α 96, β 100.4, γ 88.9°, space group *P*1), Khalilov *et al.* (1965b, Fig. 2) suggested a pattern of cation order in the third dimension of epistolite. Comparison of Figures 1 and 2 of Khalilov *et al.* (1965b) with Figure 4 of Khalilov *et al.* (1965a) indicates an epistolite structure with zig-zag chains of edge-sharing (TiO_6) octahedra alternating with similar chains of (NaO_6) octahedra. The resulting stoichiometry is in accord with their proposed formula for epistolite, $Na_2\ Ti^{4+}_2\ [Nb_2O\ _2(OH)_4]\ (Si_2O_7)_2\ (H_2O)_2$. More work has been done on the crystal structure of murmanite (Khalilov *et al.* 1965b, Rastsvetaeva & Andrianov 1986, Khalilov 1989). Its original chemical formula was given as $Na_2\ Mn\ Ti^{4+}\ [Ti^{4+}_2(OH)_4]\ [Si_2O_7]_2\ (H_2O)_4$ (Khalilov *et al.* 1965b), but has since been changed to $Na_4\ Ti^{4+}_4\ (Si_2O_7)_2\ O_4\ (H_2O)_4$ on the basis of a more recent crystal-structure refinement (Khalilov 1989). This later formula is in accord with the analytical work of Karup-Møller (1986b). From the findings of Khalilov (1989), it has been assumed that epistolite and murmanite have the same structure topology, differing only in the distribution of Ti^{4+} and Nb over the *M* sites. In later publications, epistolite has been often considered as a Nb-analogue of murmanite (*e.g.,* Egorov-Tismenko & Sokolova 1990, Ercit *et al.* 1998).

In the 1980s, A.D. Khalilov discussed with ES the possibility of refining the crystal structure of epistolite, but could not find an appropriate single crystal. It is widely known that epistolite does not form single crystals; it occurs as intergrowths with other minerals (Karup-Møller 1986a) or twinned crystals (Ferraris & Németh 2003). However, the very careful analytical and textural work of Karup-Møller (1986b) is not in accord with the formula proposed by Khalilov *et al.* (1965b), and Dr. Karup-Møller kindly supplied the best-quality material from his careful study. We emphasize that this material is very difficult to work with, and solution of the crystal structure was a non-trivial enterprise. However, we have obtained a stereochemical model of epistolite that fits the diffraction data tolerably well and is in accord with the available chemical data, and report it here.

EXPERIMENTAL

Electron-microprobe analysis

Three crystals of epistolite were analyzed with a Cameca SX–100 electron-microprobe operating in wavelength-dispersion mode with an accelerating voltage of 15 kV, a specimen current of 10 nA, a beam size of 20 μm, and count times on peak and background of 2 and 10 s, respectively. The following standards and crystals were used for *K* or *L* X-ray lines: F, P: apatite; Na, Si: tugtupite; Mg: forsterite; Ca: diopside; K: eifelite; Nb, Mn: $MnNb_2O_6$; Ti: TiO_2; Fe: fayalite; Zn: gahnite; Sr: strontianite; Zr: zircon; Ba: barite; Ta: manganotantalite. Data were reduced using the φ(ρZ) procedure of Pouchou & Pichoir (1985). The chemical composition of epistolite is given in Table 1 and is the mean of 10 determinations. The empirical formula (Table 1) was calculated on the basis of 4 Si *apfu* (atoms per formula unit), and the end-member composition is $Na_4 Nb_2 Ti^{4+} (Si_2O_7)_2 O_2 (OH)_2 (H_2O)_4$. We did not assign the small amounts of K and P in the chemical composition to the empirical formula of epistolite (Table 1), as these constituents may belong to the unidentified submicroscopic phase that has been observed in epistolite crystals from several localities (Karup-Møller 1986a).

CRYSTAL STRUCTURE

A single crystal of epistolite was mounted on a Bruker *P*4 automated four-circle diffractometer equipped with graphite-filtered Mo*K*α X-radiation and a Smart 1K CCD detector. The intensities of 4748 reflections with $\bar{6} < h < 7$, $\bar{7} < k < 10$, $\overline{16} < l < 16$ were collected to 59.99°2θ using 30 s per 0.1° frame, and an empirical absorption correction (SADABS, Sheldrick 1998) was applied. The refined unit-cell parameters (Table 2) were obtained from 2363 reflections with $I > 10\sigma I$.

On the basis of 1986 unique observed reflections ($F_o > 4\sigma F$), the crystal structure of epistolite was solved and refined with the Bruker SHELXTL Version 5.1 system of programs (Sheldrick 1997) to R_1 = 9.8% and a GoF of 1.145. Scattering curves for neutral atoms were taken from the International Tables for Crystallography (1992). *R* indices are given in Table 2, and are expressed as percentages. Site occupancies for the *M* and *A* sites were refined with the scattering curves of Nb, Ti and Na. At the last stages of the refinement, three peaks (with magnitudes from 7.6 to 2.5 e^-) were found in the difference-Fourier map, close to the *M*(1), *Si*(1) and *Si*(2) sites (1.40, 1.58 and 1.32 Å, respectively), each shifted from the corresponding site along the *b* axis. These subsidiary sites were included in the refinement, and their site occupancies were refined with the scattering curves of Nb and Si, and with U_{iso} fixed at 0.05 Å^2. The refined site-occupancies are approximately 10% of the occupancies at the associated sites. We tried to find coordination polyhedra around these partly occupied cation sites, but had no success. This is not surprising, considering the expected scattering values (approximately 10% of an O atom, ~1 e^-) and the high *R* index of the refinement. The three cation sites with ~10% occupancy presumably belong to the submicroscopic phase that is intergrown with epistolite (*cf.* Karup-Møller 1986a). Details of the data collection and structure refinement are given in Table 2, final atom parameters for the epistolite structure are given in Table 3 and for the subsidiary sites in Table 4, selected interatomic distances and angles in Table 5, refined site-scattering values and assigned populations for selected sites are given in Table 6, bond-valence values are given in Table 7, and a proposed scheme of hydrogen bonding is given in Table 8. A table of structure factors may be obtained form the Depository of Unpublished Data, CISTI, National Research Council, Ottawa, Ontario K1A 0S2, Canada.

TABLE 1. CHEMICAL COMPOSITION (wt.%)* AND UNIT FORMULA (*apfu*) FOR EPISTOLITE

SiO_2	29.59	Si	4.00
Nb_2O_5	31.43	Σ	4.00
TiO_2	10.24		
MnO	0.34	Nb	1.92
Fe_2O_3	0.35	Ti^{4+}	1.04
Ta_2O_5	0.28	Fe^{3+}	0.04
Na_2O	14.45	Σ*M*	3.00
CaO	1.89		
K_2O	0.27	Na	3.79
P_2O_5	0.36	Ca	0.27
F	1.32	Mn^{2+}	0.04
H_2O **	10.46	Σ*A*	4.06
Total	100.43	F	0.56
		(OH)	1.44
		(H_2O)	4

* MgO, ZnO, SrO, ZrO_2, BaO were not detected; 0.05 K and 0.04 P (*apfu*) are attributed to another phase.
** calculated from structure refinement

TABLE 2. MISCELLANEOUS REFINEMENT DATA FOR EPISTOLITE

a (Å)	5.460(1)
b	7.170(1)
c	12.041(2)
α (°)	103.63(3)
β	96.01(3)
γ	89.98(3)
V (Å^3)	455.4(5)
Space group	$P\bar{1}$
Z	1
Absorption coefficient (mm^{-1})	2.24
F(000)	395.0
$D_{calc.}$ (g/cm^3)	2.987
Crystal size (mm)	0.01 x 0.10 x 0.12
Radiation/ filter	Mo*K*α/graphite
2θ-range for data	59.99
R(int) (%)	6.8
Reflections collected	4748 4033
Independent reflections $F_o > 4\sigma\vert F\vert$	2495 1986
Refinement method	Full-matrix least-squares on F^2, fixed weights proportional to $1/\sigma F_o^2$
Goodness of fit on F^2	1.145
Final *R*(obs) (%) [$F_o > 4\sigma\vert F\vert$]	9.8
R indices (all data) (%)	R_1 = 12.5 WR_2 = 24.0 GoF = 1.145

DESCRIPTION OF THE STRUCTURE

Cation sites

In the crystal structure of epistolite, there are two tetrahedrally coordinated sites occupied by Si with a grand <Si–O> distance of 1.617 Å. There are two octahedrally coordinated *M* sites. The *M*(1) site is surrounded by five O atoms and one (H_2O) group, and is occupied primarily by Nb with minor amounts of Fe^{3+} and Ti^{4+} (Table 6) with <*M*(1)–O, H_2O> = 2.01 Å. The *M*(2) site is occupied solely by Ti^{4+} and is coordinated by five O atoms and an (OH) group with <*M*(2)–O,OH> = 1.962 Å. There are three *A* sites, occupied primarily by Na with minor amounts of Ca and Mn^{2+}. The *A*(1) site is octahedrally coordinated by O atoms and (OH) groups, with <*A*(1)–O,OH> = 2.34 Å. The *A*(2) site is octahedrally coordinated solely by O atoms with <*A*(2)–O> = 2.449 Å. The *A*(3) site is [8]-coordinated by six O atoms, one (OH) group and one (H_2O) group, with <*A*(3)–O, OH, H_2O> = 2.57 Å. The refined site-scattering value for *A*(3) is 16.7(6) *epfu* (electrons per formula unit), indicating that this site is only partly occupied by Na. Based on the chemical analysis (Table 1), we assigned Ca and Mn^{2+} to the *A*(3) site: 0.87 Na + 0.82 □ + 0.27 Ca + 0.04 Mn *apfu* (Table 6).

Examination of Table 6 shows that there are some significant discrepancies between the refined site-scattering values and the corresponding values derived from results of the electron-microprobe analysis. In particular, the *M*(1) site shows a refined value (74.5 *e*) much less than that required by the chemical composition derived from the microprobe results (80.6 *e*). The refined site-scattering values reflect the chemical composition

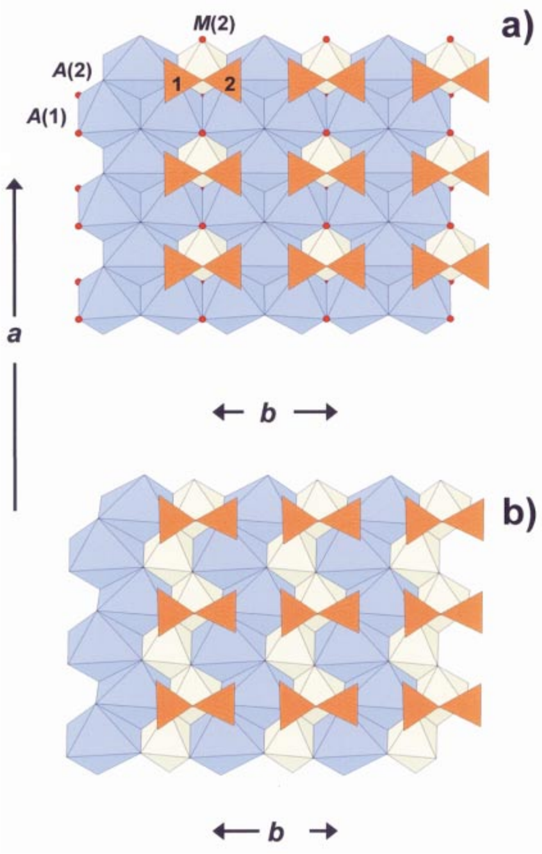

FIG. 1. General view of a sheet of octahedra with adjacent [Si_2O_7] units in (a) epistolite, and (b) murmanite. (TiO_6) octahedra are yellow, (NaO_6) octahedra are blue, (SiO_4) tetrahedra are orange, (OH) groups are shown as small red circles.

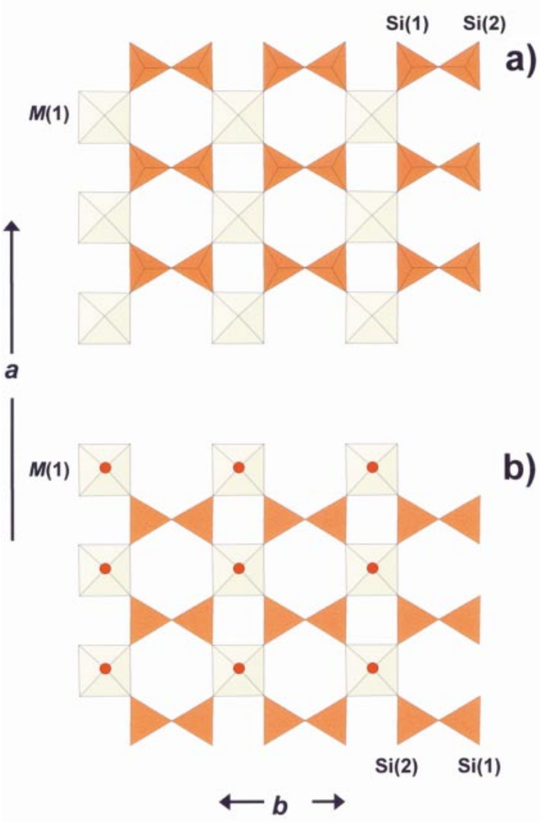

FIG. 2. Linkage of *M*(1) octahedra and [Si_2O_7] groups in the sheet of heteropolyhedra in epistolite [*A*(3) cations are omitted for clarity]: (a) the side facing a sheet of octahedra; (b) the side facing away from the sheet of octahedra. Legend as in Figure 1, (H_2O) groups are shown as large red circles.

of epistolite, whereas the chemical composition incorporates epistolite *plus the intergrown phase* represented by the *M*(1)-, *Si*(1)- and *Si*(2)-satellite peaks in our difference-Fourier map (see above) and the submicroscopic phase intergrown with epistolite that was noted in the very careful work of Karup-Møller (1986a). Hence the observed difference between the two *M*(1) site-scattering values indicates that the submicroscopic phase is more enriched in heavy species (presumably Nb and perhaps Ti) than epistolite.

Structure topology

We will describe the crystal structure of epistolite and compare it with that of murmanite to show that their structures are significantly different. In the crystal structure of epistolite, (SiO_4) tetrahedra link together to form $[Si_2O_7]$ groups. The *M*(2) (= Ti^{4+}) and *A*(1,2) (= Na) octahedra all share six common edges to form a close-packed sheet (Fig. 1a), with an *A:M* ratio of 3:1. In the crystal structure of murmanite, Ti^{4+} octahedra and Na octahedra both form edge-sharing brookite-like chains within a sheet of the same topology (Khalilov 1989) (Fig. 1b). The sheet of octahedra is a central part of the *TS* (titanium silicate) block that is a constituent of several Ti-silicate minerals (Sokolova & Hawthorne 2001). Two outer parts of the block are heteropolyhedral sheets of $[Si_2O_7]$ groups and *M*(1) octahedra (Figs. 2a, b), with large hexagon-shaped interstices that incorporate [8]-coordinated *A*(3) cations. Two heteropolyhedral sheets are connected to a sheet of octahedra *via* (a) common vertices of (SiO_4) tetrahedra and *M*(2) octahedra, and (b) linkage of *M*(1) and *A*(3) polyhedra with *A*(1) and *A*(2) octahedra (Fig. 3a). The opposite side of the sheet

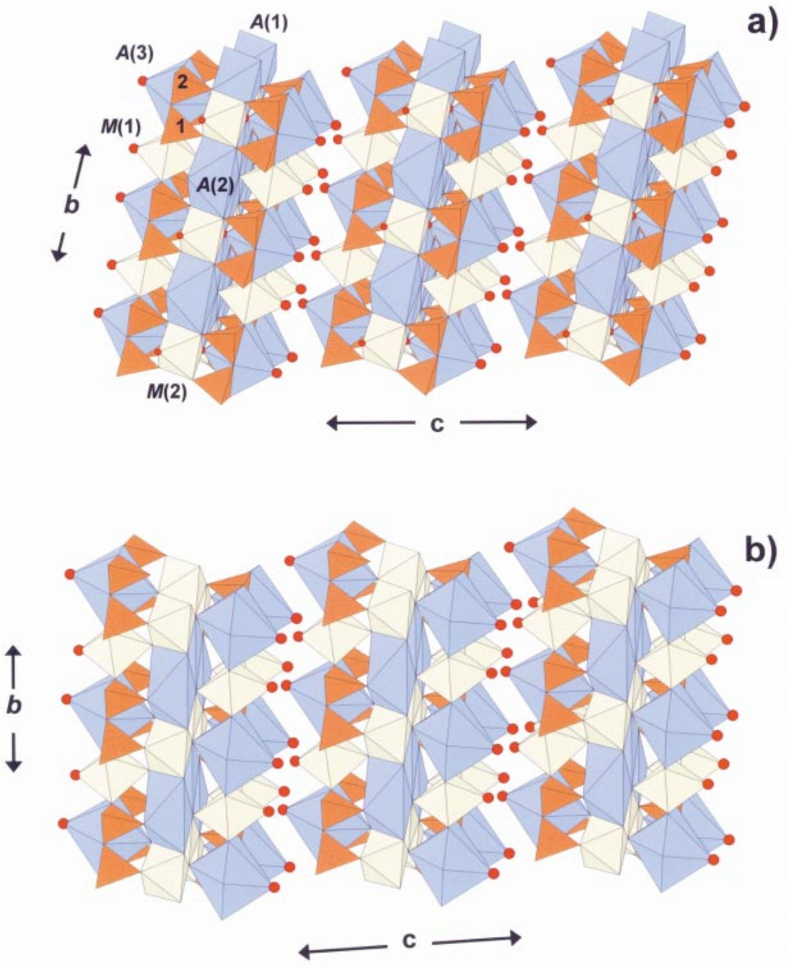

FIG. 3. General view of the crystal structure of (a) epistolite; (b) murmanite. Legend as in Figure 1; [6]- and [8]-coordinated Na polyhedra are blue.

TABLE 3. FINAL ATOM POSITIONS AND DISPLACEMENT PARAMETERS (Å^2) FOR EPISTOLITE

	x	y	z	U_{eq}	U_{11}	U_{22}	U_{33}	U_{23}	U_{13}	U_{12}
M(1)	0.7033(2)	0.60465(15)	0.25966(9)	0.0077(4)	0.0061(5)	0.0077(5)	0.0095(5)	0.0028(3)	−0.0004(3)	−0.0008(3)
M(2)	0	0	0	0.0175(8)	0.0196(16)	0.0096(14)	0.0217(16)	0.0054(11)	−0.0094(12)	−0.0025(11)
A(1)	0.5006(9)	0.2440(7)	−0.0000(4)	0.0178(11)	0.013(2)	0.017(2)	0.024(3)	0.005(2)	0.0033(19)	−0.0009(18)
A(2)	0	1/2	0	0.023(3)	0.023(5)	0.023(5)	0.025(5)	0.006(3)	0.012(3)	−0.001(3)
A(3)	0.2853(13)	−0.1172(11)	−0.2975(7)	0.026(3)	0.022(4)	0.027(4)	0.027(4)	0.004(3)	0.000(3)	−0.003(3)
Si(1)	−0.1954(6)	0.1152(4)	−0.2368(3)	0.0102(7)	0.0106(14)	0.0086(14)	0.0117(14)	0.0034(11)	0.0001(10)	0.0002(10)
Si(2)	0.1947(6)	0.3064(4)	0.2364(3)	0.0106(7)	0.0080(14)	0.0093(14)	0.0143(15)	0.0033(11)	−0.0003(10)	−0.0000(10)
O(1)	0.4530(17)	0.4206(15)	0.2788(8)	0.0211(19)	0.016(4)	0.020(4)	0.027(5)	0.010(4)	−0.009(3)	−0.014(3)
O(2)	0.4546(17)	0.8090(15)	0.2812(9)	0.027(2)	0.014(4)	0.036(6)	0.028(5)	0.006(4)	−0.002(4)	0.006(4)
O(3)	0.2084(17)	0.1165(12)	0.2896(7)	0.0175(18)	0.028(5)	0.008(4)	0.019(4)	0.007(3)	0.003(4)	0.000(3)
O(4)	0.1597(16)	−0.1589(12)	0.0984(7)	0.0155(17)	0.023(4)	0.012(4)	0.011(4)	0.001(3)	0.004(3)	0.001(3)
O(5)	−0.0375(17)	0.4228(14)	0.2861(8)	0.0211(19)	0.018(4)	0.023(5)	0.020(4)	0.002(4)	0.003(3)	0.003(3)
O(6)	0.1586(17)	0.2380(12)	0.0971(7)	0.0167(17)	0.022(4)	0.010(4)	0.018(4)	0.000(3)	0.006(3)	−0.000(3)
O(7)	0.0316(18)	0.1933(14)	−0.2897(8)	0.025(2)	0.025(5)	0.028(5)	0.022(5)	0.006(4)	0.007(4)	−0.011(4)
O(8) (OH)	0.2750(13)	−0.0371(11)	−0.0928(7)	0.0103(15)	0.004(3)	0.012(4)	0.015(4)	0.003(3)	0.001(3)	−0.000(3)
O(9)	0.6844(16)	0.5436(13)	0.1079(7)	0.0184(18)	0.017(4)	0.024(4)	0.013(4)	0.000(3)	0.003(3)	0.001(3)
O(10) (H_2O)	0.736(3)	0.6799(19)	0.4619(10)	0.043(3)	0.056(8)	0.049(7)	0.022(5)	0.002(5)	0.008(5)	0.004(6)
O(11) (H_2O)	0.255(3)	−0.263(3)	−0.4825(17)	0.091(6)	0.028(9)	0.173(18)	0.096(13)	0.078(13)	0.010(9)	−0.000(10)

TABLE 4. FINAL SUBSIDIARY ATOM POSITIONS AND ISOTROPIC DISPLACEMENT PARAMETERS (Å^2)

	Site occupancy	x	y	z	U_{iso}
M(11)	0.1	0.700(4)	0.799(3)	0.2568(16)	0.05
Si(11)	0.1	0.447(13)	1.003(10)	0.274(6)	0.05
Si(21)	0.1	0.181(14)	0.490(11)	0.236(6)	0.05

is shown in Figure 2b: (H_2O) groups of *M*(1) octahedra and *A*(3) polyhedra form the outer boundary of the *TS* blocks. Note that several types of linkages within a *TS* block have been recently described by Christiansen *et al.* (1999).

There is one unique *TS* block per unit cell in the crystal structures of epistolite (Fig. 3a) and murmanite (Fig. 3b). The blocks repeat along the *c* direction and are connected by hydrogen bonds between (H_2O) groups and O atoms of adjacent *TS* blocks. The *TS* block is a fundamental building block (*FBB*) for both epistolite and murmanite, but the topologies of the blocks are different in the two structures. This difference results from different linkage of the central sheet of octahedra to adjacent heteropolyhedral sheets. In epistolite, two [Si_2O_7] groups, one from each heteropolyhedral sheet, link to a single *M*(2) octahedron of the central sheet, and heteropolyhedral sheets are approximately related by a pseudo-mirror plane (Figs. 4a, 5a). In murmanite, two [Si_2O_7] groups, one from each heteropolyhedral sheet, link to two distinct octahedra, *Ti*(2) and *Ti*(4) (Khalilov 1989) of the brookite-like chain (Fig. 4b). Hence, heteropolyhedral sheets are shifted relative to each other in the (110) plane by about 1.1 Å (Fig. 5b). Thus the bond topology of the *TS* block is different in epistolite and murmanite, and epistolite and murmanite are not isostructural.

TABLE 5. INTERATOMIC DISTANCES (Å) AND ANGLES (°) FOR EPISTOLITE

M(1)–O(1)		1.968(9)	*M*(2)–O(4)	x2	1.971(8)
M(1)–O(2)		1.99(1)	*M*(2)–O(6)	x2	1.969(8)
M(1)–O(5)		1.976(9)	*M*(2)–O(8)	x2	1.945(7)
M(1)–O(7)		1.99(1)	<*M*(2)–O>		1.962
M(1)–O(9)		1.768(8)			
M(1)–O(10)		2.36(1)			
		2.01			
A(1)–O(4)		2.31(1)	*A*(3)–O(1)		2.64(1)
A(1)–O(6)		2.31(1)	*A*(3)–O(2)		2.58(1)
A(1)–O(8)		2.341(9)	*A*(3)–O(3)a		2.76(1)
A(1)–O(8)a		2.333(9)	*A*(3)–O(3)c		2.71(1)
A(1)–O(9)		2.39(1)	*A*(3)–O(5)		2.61(1)
A(1)–O(9)b		2.38(1)	*A*(3)–O(7)		2.61(1)
<*A*(1)–O>		2.34	*A*(3)–O(8)		2.40(1)
			A(3)–O(11)		2.22(2)
A(2)–O(4)	x2	2.562(8)	<*A*(3)–O>		2.57
A(2)–O(6)	x2	2.543(9)			
A(2)–O(9)	x2	2.243(8)			
<*A*(2)–O>		2.449			
Si(1)–O(2)		1.61(1)	*Si*(2)–O(1)		1.604(9)
Si(1)–O(3)		1.631(9)	*Si*(2)–O(3)		1.634(8)
Si(1)–O(4)		1.612(9)	*Si*(2)–O(5)		1.607(9)
Si(1)–O(7)		1.609(9)	*Si*(2)–O(6)		1.624(9)
<*Si*(1)–O>		1.616	<*Si*(2)–O>		1.617
Si(1)–O(3)–*Si*(2)		135.6(6)			

a: $-x+1, -y, -z$; b: $-x+1, -y+1, -z$; c: $-x, -y, -z$

Structural formulae for epistolite and murmanite

We may write the structural formulae of these two minerals in terms of the components of their *TS* blocks. Consider first the sheet of octahedra; as all cation sites are filled in these minerals, these sheets must have the formula [$M_n\phi_{2n}$] (= [$M\phi_2$]$_n$), where *M* is any cation and

TABLE 6. REFINED SITE-SCATTERING VALUES (*epfu*) AND ASSIGNED SITE-POPULATIONS (*apfu*) FOR EPISTOLITE

	Site-scattering	Site population	Calculated site-scattering	$<X–\phi>_{calc.}$* Å	$<X–\phi>_{obs}$ Å
M(1)	74.5(4)	1.92 Nb + 0.04 Fe^{3+} + 0.04 Ti^{4+}	80.6	2.02	2.01
M(2)	22.0(2)	1.00 Ti^{4+}	22.0	1.99	1.962
A(1)	22.0(3)	2.00 Na	22.0	2.40	2.34
A(2)	10.1(4)	0.92 Na	10.1	2.40	2.449
A(3)	16.7(6)	0.87 Na + 0.82 □ + 0.27 Ca + 0.04 Mn^{2+}	16.0	2.54	2.57

* ionic radii from Shannon (1976)

TABLE 7. BOND-VALENCE* TABLE FOR EPISTOLITE

	Si(1)	*Si*(2)	*M*(1)	*M*(2)	*A*(1)	*A*(2)	*A*(3)	Σ
O(1)		1.05	0.85				0.08	1.98
O(2)	1.03		0.81				0.09	1.93
O(3)	0.98	0.97					0.07 0.07	2.09
O(4)	1.03			$0.63^{\times2}\downarrow$	0.25	$0.14^{\times2}\downarrow$		2.05
O(5)		1.04	0.84				0.08	1.96
O(6)		0.99		$0.64^{\times2}\downarrow$	0.25	$0.15^{\times2}\downarrow$		2.03
O(7)	1.04		0.81				0.08	1.93
O(8)				$0.68^{\times2}\downarrow$	$0.23^{\times2}\downarrow$		0.13	1.27
O(9)			1.46		$0.21^{\times2}\downarrow\rightarrow$	$0.25^{\times2}\downarrow$		2.13
O(10)			0.34					0.34
O(11)							0.19	0.19
Σ	4.08	4.05	5.11	3.90	1.38	1.08	0.79	

* bond-valence parameters (*vu*) from Brown (1981)

TABLE 8. PROPOSED HYDROGEN BONDING FOR EPISTOLITE

Species	*D*	*A*	*D–A* (Å)
OH	O(8)	O(5)	3.33(1)
H_2O	O(10)	O(3)	2.99(1)
		O(11)a	2.78(2)*
		O(11)b	2.85(2)*
H_2O	O(11)	O(7)	3.16(2)
		O(10)	3.06(3)

a: *x*, *y*+1, *z*+1; b: *x*+1, *y*+1, *z*+1;
* these bonds are mutually exclusive.

ϕ is any anion. We may write the corresponding formulae as follows: epistolite: $Na_3\,Ti^{4+}\,(OH)_2\,O_6$; murmanite: $Na_2\,Ti^{4+}_2\,O_2\,O_6$. Consider next the heteropolyhedral sheet; these have the formula $[^{[8]}A_2\,^{[6]}M_2\,(Si_2O_7)_2\,\phi_8]$; we have written here the formula of the two heteropolyhedral sheets that constitute a single *TS* block. We may write the corresponding formulae as follows: epistolite: $[^{[8]}Na\,\square\,^{[6]}Nb_2\,(Si_2O_7)_2\,O_2\,(OH)_2\,(H_2O)_4]$; murmanite: $[^{[8]}Na_2\,^{[6]}Ti^{4+}_2\,(Si_2O_7)_2\,O_2\,O_2\,(H_2O)_4]$. In terms of the constituent sheets, we may write the formulae of epistolite and murmanite in the following way:

Mineral	*Sheet of Octahedra*	*Sheets of Heteropolyhedra*
Epistolite	$Na_3Ti^{4+}(OH)_2$* O_6*	$^{[8]}Na\,\square\,Nb_2\,(Si_2O_7)_2\,O_2\,(OH)_2\,(H_2O)_4$
Murmanite	$Na_2Ti^{4+}_2O_2$* O_6*	$^{[8]}Na_2\,Ti^{4+}_2(Si_2O_7)_2\,O_2\,O_2\,(H_2O)_4$

Anions indicated by stars belong to the sheet of octahedra and adjacent sheets of heteropolyhedra, hence they should not be summed from the sheet of octahedra to give the complete formula as they are counted in the sheets of heteropolyhedra.

The corresponding end-member formulae for these two minerals are as follows:

Epistolite	$Na_4\,Nb_2\,Ti^{4+}\,(Si_2O_7)_2\,O_2\,(OH)_2\,(H_2O)_4$
Murmanite	$Na_4\,Ti^{4+}_4\,(Si_2O_7)_2\,O_4\,(H_2O)_4$

Hydrogen bonding

It was not possible to directly locate the H atoms of the (OH) and (H_2O) groups in epistolite. However, bond-valence calculations show that O(10) and O(11) are O atoms of (H_2O) groups, and O(8) is an O atom of an (OH) group (Table 7). There are four hydrogen-bonds involving four (H_2O) groups connecting two *TS* blocks (Table 8, Figs. 6a, b). To derive a possible local stereochemistry for these hydrogen bonds, we note that an O atom of an (H_2O) group usually forms four tetrahedrally arranged bonds (*i.e.*, sp^3 hybridization). Each (H_2O) group is a ligand of an *M*(1) atom [O(10)] or an *A*(3) atom [O(11)]; thus the O atom of each (H_2O) group is bonded to one cation. Hence there should be three additional bonds, two donor–hydrogen bonds of the (H_2O) group, and a third hydrogen...acceptor bond from another (H_2O) group. Figure 6a shows all possible D(donor)–A(acceptor) distances involving (H_2O) groups. There is no possibility for sp^3 hybridization-type hydrogen bonding within this arrangement of bonds constrained by $P\bar{1}$ symmetry. Thus we conclude that hydrogen bonding does not obey $P\bar{1}$ symmetry, whereas with $P1$ symmetry, a stereochemically sensible scheme can be derived (Fig. 6b). There are two (mutually exclusive) D–A bonds [O(10)–O(11)a and O(10)–O(11)b] that can each occur (Table 8). For these particular bonds, the mean *D* (donor)–*A* (acceptor) distance is 2.97 Å, corresponding to weak hydrogen-bonding. The arrangement of hydrogen bonds is shown in Table 8 and Figure 6a. There is weak hydrogen bonding involving (OH) groups within the *TS* block (Table 8, Fig. 6b), but most of the hydrogen bonds link adjacent *TS* blocks (Fig. 6b).

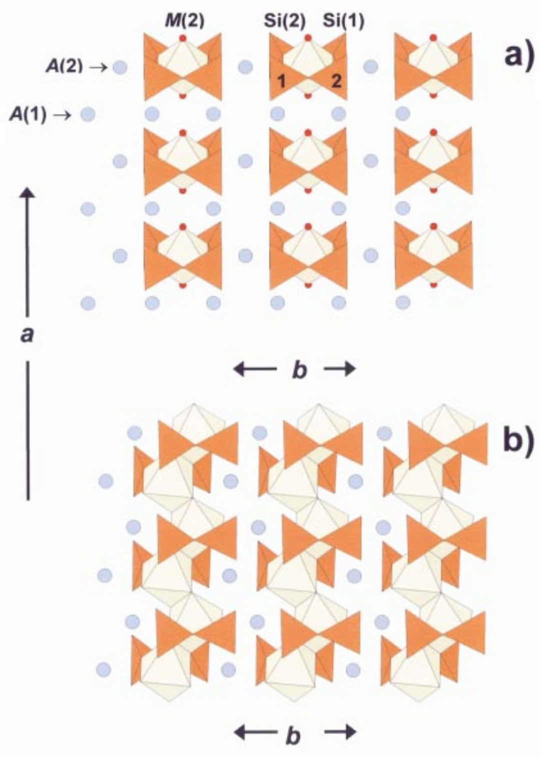

FIG. 4. Linkage of [Si_2O_7] groups of two adjacent sheets of heteropolyhedra with (TiO_6) octahedra of the central sheet in (a) epistolite, and (b) murmanite; [6]-coordinated Na atoms are shown as blue circles.

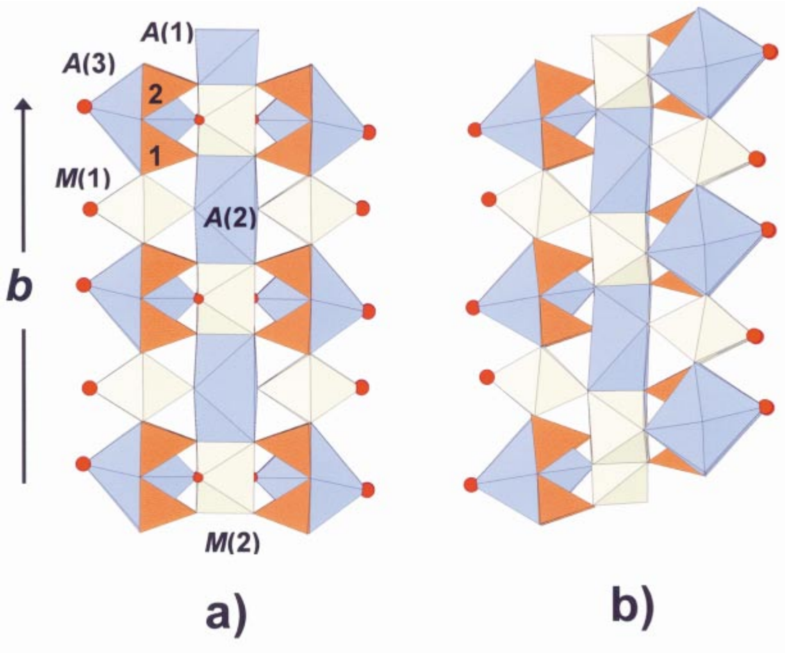

FIG. 5. Linkage of two sheets of heteropolyhedra with a sheet of octahedra within one TS block in (a) epistolite, and (b) murmanite. Legend as in Figure 3; [8]-coordinated Na atoms are shown as blue circles.

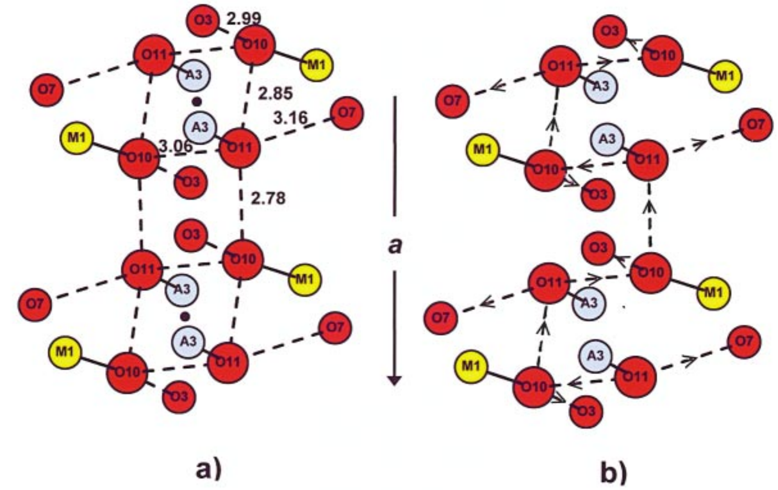

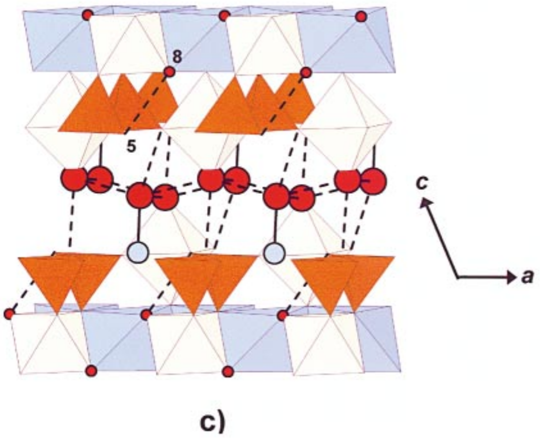

FIG. 6. Proposed scheme of hydrogen bonding in epistolite: (a) all possible D–A distances involving (H_2O) groups are shown (in Å); the black circles indicate inversion centers. (b) A general scheme of hydrogen bonding that conforms to $P1$ symmetry. (c) An *xz* projection of the crystal structure. Legend as in Figures 1 and 3; (H_2O) and (OH) groups are shown as large and small red circles, [8]-coordinated Na atoms are shown as blue circles, possible donor (D)–acceptor (A) distances are shown as dashed lines, and bonds from *A*(3) and *M*(1) atoms to (H_2O) groups are shown as solid lines. The arrows indicate the direction from donor to acceptor anions.

Some of hydrogen bonds proposed are quite long, but as shown by Brown (1976), significant interactions still occur at such distances.

SUMMARY

(1) Epistolite and murmanite are not isostructural, despite the similarity of their formulae and unit cells. The difference between them involves the topology of their main structural unit, the *TS* (titanium silicate) block.

(2) The different topologies of the *TS* blocks result from different linkages of the central sheet of octahedra with the two adjacent sheets of heteropolyhedra. In the crystal structure of epistolite, two sheets of heteropolyhedra are approximately related by a pseudomirror plane, m_z, coinciding with the plane of the sheet of octahedra. In murmanite, two sheets are shifted relative to each other.

(3) Detailed structural formulae for the *TS* block in epistolite and murmanite (Khalilov 1989) are as follows:

Mineral	*Sheet of Octahedra*	*Sheets of Heteropolyhedra*
Epistolite	Na_3 Ti^{4+} $(OH)_2$* O_6*	$^{[8]}Na$ □ Nb_2 $(Si_2O_7)_2$ O_2 $(OH)_2$ $(H_2O)_4$
Murmanite	Na_2 $Ti^{4+}{}_2O_2$* O_6*	$^{[8]}Na_2$ $Ti^{4+}{}_2$ $(Si_2O_7)_2$ O_2 O_2 $(H_2O)_4$

Anions indicated by stars belong to the sheet of octahedra and adjacent sheets of heteropolyhedra, hence they should not be summed (from the sheet of octahedra) to give the complete formula as they are counted in the sheets of heteropolyhedra.

(4) The ideal (end-member) chemical formula of epistolite is Na_4 Nb_2 Ti^{4+} $(Si_2O_7)_2$ O_2 $(OH)_2$ $(H_2O)_4$.

(5) Murmanite and epistolite are related by the substitution $Ti^{4+}_3 + O^{2-}_2 \leftrightarrow Nb^{5+}_2 + \square + (OH)^-_2$.

(6) Local decrease of symmetry from $P\bar{1}$ to $P1$ results from hydrogen bonds of (H_2O) groups located between the TS blocks.

Acknowledgements

We thank Giovanni Ferraris in particular, Ole Johnsen, Robert T. Downs and Robert F. Martin for their comments on this paper. We are very grateful to S. Karup-Møller for a sample of epistolite from the Ilímaussaq alkaline complex, South Greenland, and to Mark Cooper for his help in finding the best possible single crystal and for collection of the X-ray data. FCH was supported by a Canada Research Chair and Major Equipment, Discovery and Major Facilities Access grants from the Natural Sciences and Engineering Research Council of Canada.

References

Bøggild, O.B. (1901): Epistolite, a new mineral. *Medd. Grønland* **24**, 183-190.

Brown, I.D. (1976): Hydrogen bonding in perchloric acid hydrates. *Acta Crystallogr.* **A32**, 786-792.

________ (1981): The bond-valence method: an empirical approach to chemical structure and bonding. *In* Structure and Bonding in Crystals II (M. O'Keeffe & A. Navrotsky, eds.). Academic Press, New York, N.Y. (1-30).

Christiansen, C.C., Makovicky, E. & Johnsen, O. (1999): Homology and typism in heterophyllosilicates: an alternative approach. *Neues Jahrb. Mineral., Abh.* **175**, 153-189.

Egorov-Tismenko, Yu.K. & Sokolova, E.V. (1990): The homologous series seidozerite–nacaphite. *Mineral. Zh.* **12**(4), 40-49 (in Russ.).

Ercit, T.S., Cooper, M.A. & Hawthorne, F.C. (1998): The crystal structure of vuonnemite, $Na_{11}Ti^{4+}Nb_2(Si_2O_7)_2(PO_4)_2O_3(F,OH)$, a phosphate-bearing sorosilicate of the lomonosovite group. *Can. Mineral.* **36**, 1311-1320.

Ferraris, G. & Németh, P. (2003): Pseudo-symmetry, twinning and structural disorder in layer titanosilicates. *Abstracts of the 21st European Crystallographic Meeting* (*Durban, South Africa*).

International Tables for X-Ray Crystallography (Vol. C) (1992): Kluwer, Dordrecht, The Netherlands.

Karup-Møller, S. (1986a): Epistolite from the Ilímaussaq alkaline complex in South Greenland. *Neues Jahrb. Mineral., Abh.* **155**, 289-304.

________ (1986b): Murmanite from the Ilímaussaq alkaline complex, South Greenland. *Neues Jahrb. Mineral., Abh.* **155**, 67-88.

Khalilov, A.D. (1965): *X-Ray Diffraction Study of the Lomonosovite – Murmanite Minerals.* Ph.D. thesis, Moscow State University, Moscow, Russia (in Russ.).

________ (1989): Refinement of the crystal structure of murmanite and new data on its crystal chemistry. *Mineral. Zh.* **11**(5), 19-27 (in Russ.).

________, Makarov, Ye.S., Mamedov, Kh.S. & P'yanzina, L.Ya. (1965b): Crystal structure of minerals of the murmanite – lomonosovite group. *Dokl. Akad. Nauk SSSR* **162**, 138-140.

________, Mamedov, Kh.S., Makarov, Ye.S. & P'yanzina, L.Ya. (1965a): Crystal structure of murmanite. *Dokl. Akad. Nauk SSSR* **161**, 150-152.

Pouchou, J.L. & Pichoir, F. (1985): "PAP" ($\phi\rho Z$) procedure for improved quantitative microanalysis. *In* Microbeam Analysis – 1985. San Francisco Press, San Francisco, California (104-106).

Rastsvetaeva, R.K. & Andrianov, V.I. (1986): New data on the crystal structure of murmanite. *Sov. Phys. Crystallogr.* **31**, 44-48.

Semenov, E.I., Organova, N.I. & Kukharchik, M.V. (1962): New data on minerals of the lomonosovite – murmanite group. *Sov. Phys. Crystallogr.* **6**, 746-751.

Shannon, R.D. (1976): Revised effective ionic radii and systematic studies of interatomic distances in halides and chalcogenides. *Acta Crystallogr.* **A32**, 751-767.

Sheldrick, G.M. (1997): *SHELX–97: Program for the Solution and Refinement of Crystal Structures.* Siemens Energy and Automation, Madison, Wisconsin.

________ (1998): *SADABS User Guide*. University of Göttingen, Göttingen, Germany.

Sokolova, E. & Hawthorne, F.C. (2001): The crystal chemistry of the $[M_3\phi_{11-14}]$ trimeric structures: from hyperagpaitic complexes to saline lakes. *Can. Mineral.* **39**, 1275-1294.

Received November 28, 2003, revised manuscript accepted March 11, 2004.